JOURNAL OF AGRICULTURAL AND FOOD CHEMISTRY

Application of FTIR Spectroscopy for the Quantification of Sugars in Mango Juice as a Function of Ripening

IOLA F. DUARTE, ANTÓNIO BARROS, IVONNE DELGADILLO, CLÁUDIA ALMEIDA, AND ANA M. GIL*

Department of Chemistry, University of Aveiro, 3810-193 Aveiro, Portugal

FTIR−ATR spectroscopy and multivariate analysis were used for quantification of sugars in mango juices as a function of ripening. Calibration was based on sucrose/glucose/fructose mixtures, with six concentration levels and following a triangular experimental design. PLS1 regression of the spectra first derivatives gave the best results, enabling quantification of fructose, sucrose, and glucose with 1.4, 1.4, and 4.9% prediction errors, respectively. Throughout ripening, sucrose and fructose were accurately quantified by PLS−FTIR, whereas the accuracy of glucose determination decreased at later stages, when concentrations fell to 0.6−1.5 g/L. These results enabled a correlation with fruit ripening stage to be established. This may be particularly useful to detect over-ripening in fresh fruits, a period when other indicators (pH and % soluble solids (SS)) do not change significantly; this knowledge may help in predicting fruit stability to transport and storage. Similar information obtained for nonfresh juices (in which pH and %SS may be masked by additives), may help determine whether the source fruits had suitable ripening stages.

KEYWORDS: Fruit; mango; juice; mid-infrared; FTIR; ATR; sugars; quantification; spectroscopy; PCA; PLS; chemometrics

INTRODUCTION

The sugar composition of fruits and its dependence upon the ripening process has been studied for many fruits, including mango. Glucose, fructose, and sucrose are the most abundant components of mango juice, and they show large variations as ripening proceeds (*1*−*5*). In fact, total sugar content is commonly used as a ripening indicator and is one of the most important criteria for evaluating the edibility of fruits and the quality of their processed products. Traditionally, sugar contents of foods (particularly in juices and beverages) are estimated based on refractive index measurements or volumetric procedures, which provide information about the total sugar content and the amount of reducing sugars (glucose and fructose), respectively (*6*). For quantifying each sugar separately, several methods can be employed, including enzymatic analysis and chromatographic methods (*7*−*9*). FTIR spectroscopy has become an alternative technique for the analysis of sugars in food samples, having the attractive features of being noninvasive and potentially more rapid than the above methods. Mid-infrared FTIR has been increasingly used, often coupled with chemometrics, to study a range of food samples (*10*−*15*) and particularly to study liquid foods such as juices and soft drinks (*16*−*21*). The development of a wide range of sampling accessories, such as attenuated total reflectance (ATR) cells, has led to major improvements by simplifying sample handling and avoiding measurement problems often found in transmission cells, such as difficulties in filling and cleaning or the variation of sample path length due to window wear. Regarding the determination of sugars in fruit juices, a study by partial least squares (PLS)−FTIR has included a comparison of the performances of the horizontal ATR cell and the cylindrical internal reflection (CIRCLE) cell, showing that the former leads to more reproducible and accurate results (*21*). In fact, many authors have illustrated the applicability of mid-FTIR ATR spectroscopy to the quantification of sugars in natural samples. Sucrose content in raw sugar cane juice samples was predicted by PCR of FTIR ATR data (*19*, *20*). Cane juice samples were used for calibration, and prediction equations were established by relating spectral data with reference polarimetric data. Although the use of real samples as a calibration set may aid in taking into account possible contributions due to the overall composition of the system, the choice of the reference analytical method may, for the same reason, be hindered by possible interferences. In addition, a calibration set based on real samples will be specifically applicable to the particular sample under study, whereas, if a suitable model can be built based on simpler laboratory samples, such a robust model may be applicable to other systems, e.g., other fruits. Therefore, some studies have been carried out based on external calibration sets prepared from aqueous standard solutions (*18*, *21*, *22*). Sugars and citric acid were quantified in synthetic mixtures and in apple juices, using PLS and PCR of FTIR ATR data. The calibration set comprised 24 standard mixtures of glucose, fructose, sucrose, and citric

* To whom correspondence should be addressed. Tel +351 234 370707, fax +351 234 370084, e-mail agil@dq.ua.pt.

10.1021/jf011575y CCC: $22.00
Published on Web 04/20/2002

acid (*22*), in which concentrations were gradually increased for all components simultaneously. Cross-validation of the methods indicated good agreement between known and predicted concentrations, and some results of the application to apple juices were shown. However, comparison with a reference method to evaluate their accuracy was lacking. The use of a reduced calibration set, comprising 8 ternary mixtures of glucose, fructose, and sucrose at two concentration levels, has been recently proposed for quantification of sugars in several fruit juices and soft drinks (*18*, *21*). The FTIR acquisition parameters were optimized in order to improve the predictive ability of the PLS model employed, and concentrations of the three sugars were estimated in standards and in some fruit juices and soft drinks.

In this work, we apply the PLS method to mid-FTIR ATR data for quantifying glucose, fructose, and sucrose in mango juices at different ripening stages. The sugar composition of mango juice during the ripening process varies significantly, typically showing a marked increase in the most abundant sugar, sucrose, and some variations in the lower contents of glucose and fructose (*2*−*5*). The aim of this work is to develop a method which takes into account the expected variation ranges for each sugar and which may be used to determine the content of each of the sugars, and, hence, the degree of ripening of the fruit from which the juice is obtained. A recently developed single-reflectance ATR cell is employed to record the FTIR spectra of both juices and sugar standard solutions. This cell enables very small sample amounts to be analyzed (enough to cover a 2-mm diameter crystal surface) and is easy to handle with respect to cell cleaning between experiments. The PLS method is constructed with a set of sucrose/glucose/fructose mixtures comprising six concentrations for each sugar, within the range of concentrations expected during ripening. The concentrations predicted for mango juices by PLS−FTIR are compared with results obtained by enzymatic analysis of the same samples, so that the accuracy of the predicted values can be evaluated. Finally, the relationships between ripening stage and spectral data, firmness values, and enzymatic and chemical analyses are discussed, regarding the use of each of these measurements as ripening indicators.

MATERIALS AND METHODS

Standard Solutions. Standard solutions of glucose, fructose, and sucrose were prepared from analytical grade reagents obtained from Sigma-Aldrich. The calibration set was composed of 1 solution of each sugar, 9 binary mixtures, and 10 ternary mixtures, prepared according to a triangular experimental design. Six concentration levels were chosen for each sugar, based on the concentration ranges commonly found in mango juices at different ripening stages (*2*, *3*, *23*): sucrose, 4−148 g/L; glucose, 3−59 g/L; fructose, 4−99 g/L. **Table 1** shows a listing of the standard mixtures prepared and respective sugar concentrations.

Mango Juices. Mangoes of the Tommy Atkins cultivar, grown in Brazil, were ripened at 22 ± 1 °C during 23 days. The degree of ripening was monitored by color and firmness so that the fruits on day 1 were characterized by high firmness, green/red skin, and light yellow pulp; on day 5, by slightly softer texture, some yellow spots on the skin, and yellow pulp; on day 9, by soft texture, yellow/red skin, and intensely yellow pulp; from day 11 onward, by all the latter properties, which gradually increase in intensity. Periodically, three fruits were randomly selected for analysis, and their firmness was measured using a texturometer. The pulps of the selected fruits were macerated separately in a domestic juice extractor, centrifuged during 15 min at 15000 rpm, and filtered through a glass microfiber filter, under vacuum. To prevent microbial growth, sodium azide was added so that each sample contained an azide concentration of 0.05%. The samples were frozen in liquid nitrogen and stored at −20 °C until FTIR analysis was performed on the thawed samples. The three juices collected at each ripening day were mixed together to give samples of average composition (i.e., more representative of each ripening stage) and their FTIR spectra were recorded. To our knowledge, no systematic study has been carried out to establish the medium- and long-term effects of storage at −20 °C on the samples; however, measurements of pH and soluble solids indicated that no significant changes occurred under the conditions of this work (storage during up to 12 weeks).

Table 1. Concentrations (g/L) of the Three Sugars in the Standard Solutions of the Calibration Set

	sugar concentration (g/L)		
standard solution no.	glucose	fructose	sucrose
1	2.96	4.45	88.90
2	7.41	4.45	59.26
3	2.96	29.64	59.26
4	14.82	4.45	29.63
5	7.41	29.64	29.63
6	2.96	44.46	29.63
7	29.64	4.45	4.45
8	14.82	29.64	4.45
9	7.41	44.46	4.45
10	2.96	59.28	4.45
11		4.45	118.53
12		29.64	88.90
13		59.28	29.63
14	2.96	74.10	
15	7.41	59.28	
16	29.64	29.64	
17	44.46		4.45
18	29.64		29.63
19	7.41		88.90
20			148.16
21		98.80	
22	59.28		

FTIR Spectroscopy. Fourier transform infrared spectra of standard solutions and of juice samples were collected on a Bruker IFS55 FTIR spectrometer. A single reflectance horizontal ATR cell (Golden Gate, equipped with a diamond crystal) was used. The data were recorded at 20 ± 1 °C, in the spectral range of 700−4000 cm^{-1}, by accumulating 512 scans with a resolution of 4 cm^{-1}, as recommended by a previous study of FTIR acquisition conditions and their effect on mean error of prediction (MEP) values (*18*). For each sample, a total of five spectra were recorded (named here as replica spectra), with each spectrum obtained for a different sample batch. Between determinations, the crystal was carefully cleaned with water, and, to avoid memory effects, the replica spectra were recorded nonconsecutively (i.e., intermingled with the spectra of other samples). In this way, 110 spectra of standard solutions and 40 spectra of juices were recorded. The first derivatives of the region 1250−900 cm^{-1} region were used for the multivariate data analysis, based on a comparison of data obtained from analysis of raw spectra and 1st and 2nd derivatives of the spectra, as described in the Results and Discussion section.

Texture, pH, % Soluble Solids, and Enzymatic Tests. At each ripening stage, firmness measurements were performed on the three selected fruits using a texture analyzer TA-Hdi. The compression force applied to the unpeeled pulp during 15 s was recorded in 12 points along the equatorial ring of each fruit. An average value of force (g) was calculated for each day, based on the values obtained for the three fruits at the same ripening stage. As pH and % soluble solids (%SS) are usual indicators used for the characterization of juices (*6*, *24*), these were measured (with precisions ±0.01 and ±0.2%, respectively) for each juice sample. To test the accuracy of the PLS−FTIR sugar quantification in mango juices, each of the sugars was quantified enzymatically for a selected set of samples, using the triple test for sucrose/D-glucose/D-fructose and the single test for D-glucose, both purchased from Boehringer Mannheim. For the earlier days of ripening the triple test was employed, whereas for ripening stages later than day 13 the glucose-specific test was used because glucose content becomes much lower than that of the other sugars.

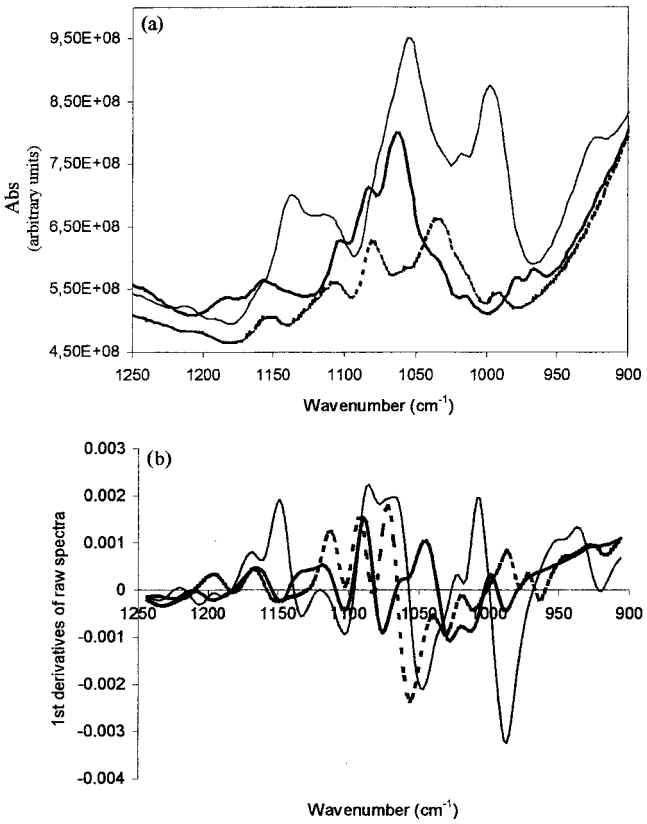

Figure 1. (a) FTIR spectra (1250–900 cm^{-1}) of standard aqueous solutions of sucrose (—), glucose (- - - -), and fructose (—), recorded using a Golden Gate single reflectance ATR cell, resolution: 4 cm^{-1}. (b) First derivative functions of the FTIR spectra shown in (a).

Principal Components Analysis (PCA) and Partial Least Squares (PLS) Regression. As described in the literature, PCA is used to find the main variability sources in a data set and the relationship between/within objects and variables; further details about the method may be found in ref *25*. PLS is used to model the relationship between a set of predictor variables X (n objects × k variables) and a set of response variables Y (n objects × m responses) (*26*). In this study there is only one response (sugar concentration), therefore Y has [n objects × 1 response] dimensions. Based on the PLS model, the sugar contents were predicted with prediction errors defined as % root mean square error of prediction (RMSEP):

$$\text{RMSEP (\%)} = \frac{100}{\bar{y}}\left(\sqrt{\frac{\sum_{i=1}^{N}(y_i - \hat{y}_i)^2}{N}}\right)$$

where N = number of samples, y_i = actual concentration, $\hat{y}_i$ = predicted concentration, and $\bar{y}$ = average of actual concentration values.

RESULTS AND DISCUSSION

Sugar Quantification in Standard Solutions by PLS−FTIR. Glucose, fructose, and sucrose show intense and characteristic bands in the fingerprint region (1250−900 cm^{-1}) of the mid-infrared wavelength range (**Figure 1a**). The plots of the first derivative functions of each spectrum are also shown (**Figure 1b**). It is clear from both plots that when the three sugars are present in the same solution, strong band overlap occurs and seriously hinders individual sugar identification/quantification. For a better understanding of the main sources of variability affecting the FTIR spectra of the standard sugar solutions used for calibration in this work, a principal component analysis (PCA) was performed for the 1250−900 cm^{-1} region of the corresponding spectra. **Figure 2a** shows the scores scatter plot of the two first principal components (PCs), which together account for 99% of the total variability present in the spectra. The plot obtained shows that the samples are suitably distributed along a concentration gradient, according to their sugar composition determined by the triangular experimental design employed. As expected, the three individual sugar solutions at maximum concentration levels are located at the vertexes of the "triangle": sucrose is located in the negative side of PC1 axis while glucose and fructose are located in the positive side of PC1. This distinction can be further interpreted by inspecting

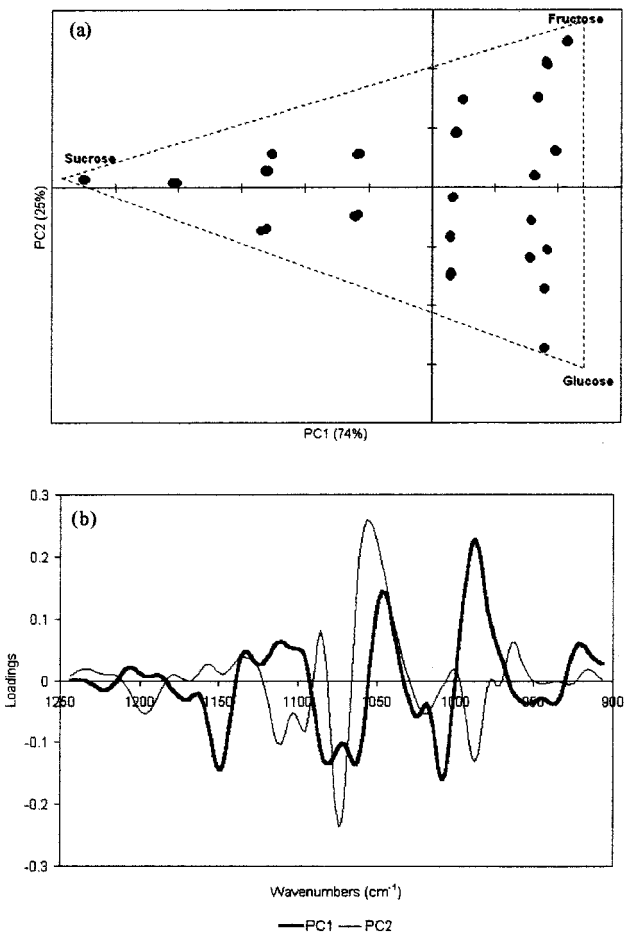

Figure 2. (a) Scores scatter plot of the two first principal components, PC1 and PC2, obtained for the set of standard sugar solutions. (b) Loadings profiles obtained for PC1 and PC2.

Table 2. Statistical Results of the Application of PLS1 to the Three Sets of Data: Raw Spectra, First Derivative Spectra, and Second Derivative Spectra

	latent variables	RMSEP (%)
	Autoscaled Raw Spectra	
fructose	8	9.3
glucose	5	10.1
sucrose	7	14.9
	First Derivative Spectra	
fructose	4	1.4
glucose	4	4.9
sucrose	4	1.4
	Second Derivative Spectra	
fructose	4	3.0
glucose	6	5.7
sucrose	6	1.8

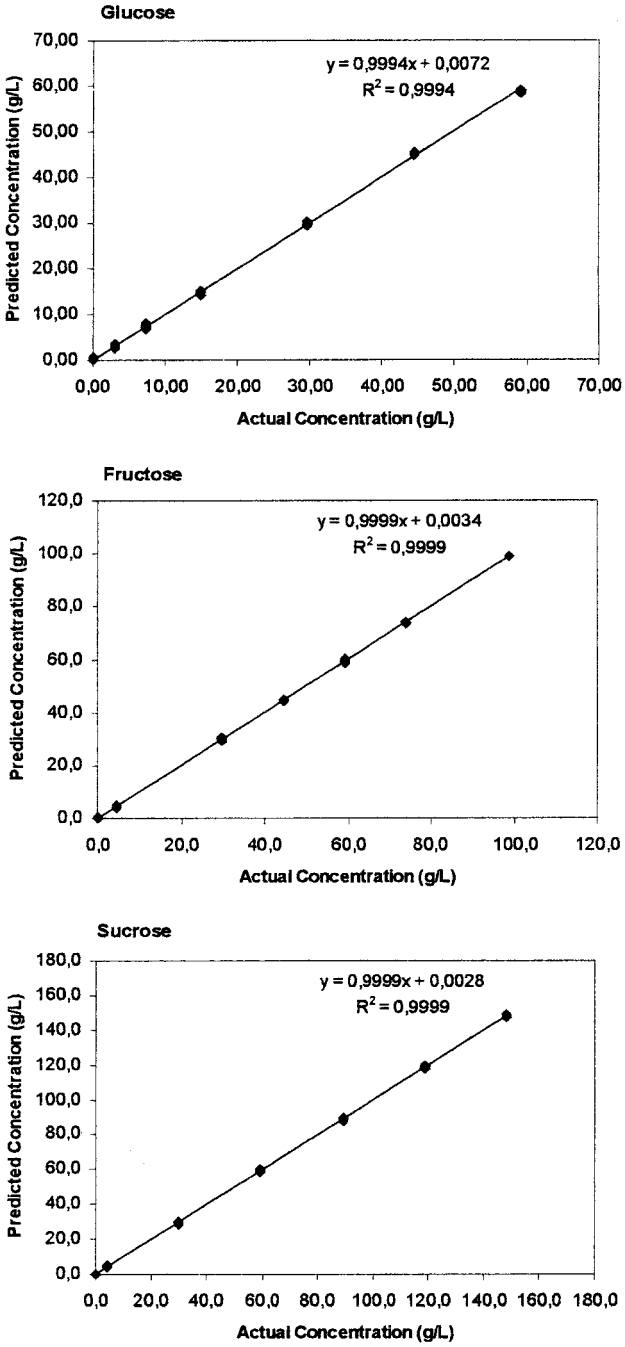

Figure 3. Calibration curves for glucose, fructose, and sucrose, obtained by PLS of the FTIR spectra of the standard solutions.

the loadings corresponding to PC1 (**Figure 2b**). It can be seen that the bands related to sucrose (negative PC1 loadings) are those at 1149, 1080, 1062, 1024, 1008, 956, and 937 cm^{-1}. Comparison with the first derivative spectra shown in **Figure 1b** confirms that these are indeed the main bands characteristic of sucrose. On the other hand, the bands located on the positive side of PC1, at 1134, 1109, 1045, 987, and 920 cm^{-1}, relate to the variations of the monosaccharide sugars fructose and glucose. The scores scatter plot (**Figure 2a**) also shows a distinction between fructose and glucose along the PC2 axis: positive PC2 for fructose and negative PC2 for glucose. Indeed, the positive bands at 1086, 1055, and 962 cm^{-1} (**Figure 2b**) are characteristic of fructose, whereas those at 1111, 1095, 1072, 1018, and 987 cm^{-1} arise from glucose.

PLS1 regression was applied to the raw spectra (autoscaled, centered, and standardized), to the first derivatives of the spectra,

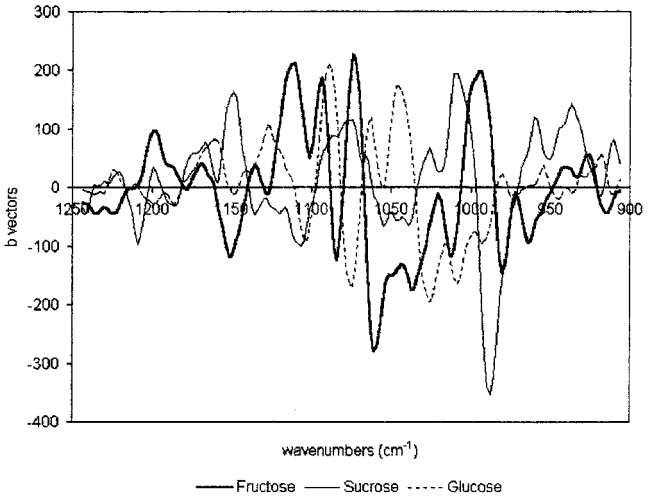

Figure 4. **b** vectors obtained with the PLS1 regression model, with four latent variables, for sucrose (—), glucose (- - - -), and fructose (**—**).

and to the second derivatives of the spectra. The derivatives were calculated based on the Savistsky−Golay (SG) procedure, using a 2nd degree polynomial with seven points (2*3 + 1) (*27*). **Table 2** shows the statistical parameters obtained for the three models. Each model was tested by internal cross-validation, leaving out one of the samples (i.e., all its 5 replica spectra) and treating it as an unknown sample. The objective function used to find the "best" model was the root mean square error of cross-validation (RMSECV), in percentage. It is clear from the lower RMSEP values (**Table 2**) that the best results were obtained for the first derivative spectra; **Figure 3** shows the calibration curves obtained for each of the three sugars. A similar observation had been noted in a previous study in which raw spectra and first derivatives were considered (*18*). Indeed, the errors and the model dimensionalities (or latent variables) corresponding to the first derivative treatment are lower than those obtained for the remaining data pretreatments, particularly that of the raw absorbance spectra. Therefore, the underlying variations present in the overlapped FTIR spectra of sucrose, glucose, and fructose mixtures are most suitably identified with the use of the first derivatives of the spectra, as these seem to highlight the differences between sugars and eliminate baseline drift effects. In addition, it also becomes clear from **Table 2** that the error obtained for glucose is higher than those obtained for sucrose and fructose. This may be a reflection of the relatively low glucose concentrations, spread within a narrower range (3−59 g/L) than those of sucrose and fructose (4−148 and 4−100 g/L, respectively).

Figure 4 illustrates the **b** vectors for each sugar as obtained from the PLS1 regression procedure. These vectors establish the profile of each sugar and enable the amount of each sugar to be predicted in test or real samples. All three obtained PLS1 models (each with 4 latent variables) explained 99% of the variability present in the concentration vectors (sugars amount).

Effect of Ripening on Mango Fruit and Juices. *General Physical and Chemical Changes.* **Figure 5** shows the changes in firmness of the mango fruit during ripening, as well as the changes in pH and %SS (reflecting amount of total sugars) observed for the corresponding juices. For each ripening stage, the values obtained for each of the three mango fruits give an indication of the natural compositional variability of the fruits. This variability is, in each ripening day, of the order or larger than the measurements precision (see Materials and Methods) and it can be seen that, with the exception of day 7, the variability between different fruits is lower than the overall

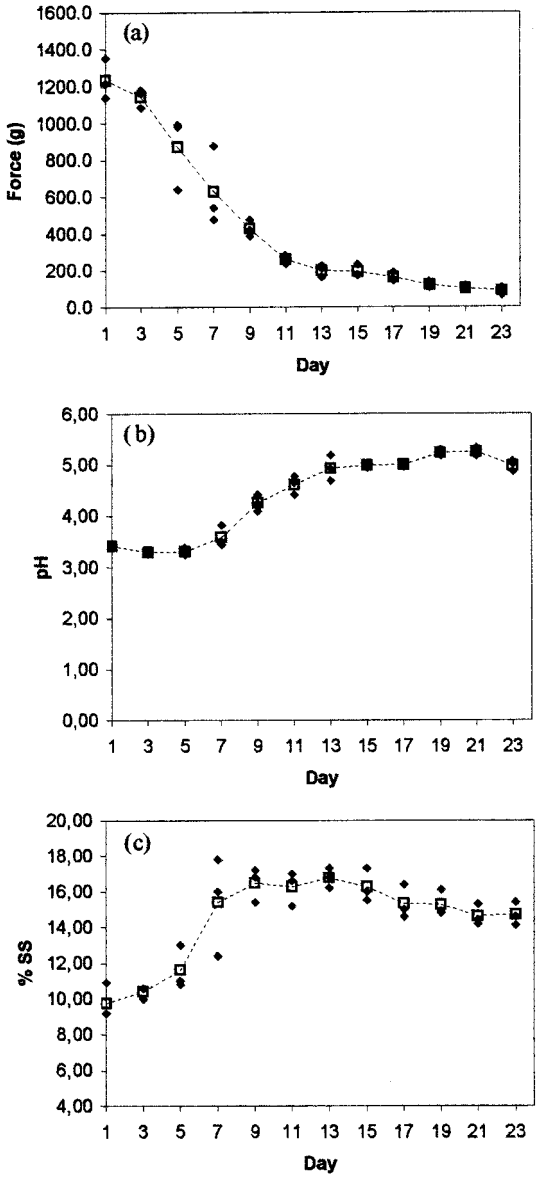

Figure 5. Changes in (a) fruit firmness, measured as force (g); (b) juice pH; and (c) juice %SS, as a function of ripening. The symbols (◆) indicate the values for each of the three fruits selected for each day; the dashed curve is defined by the average values (□).

changes (in firmness, pH, and %SS) induced by ripening. As expected, firmness decreases consistently until the fruit is ready to eat, on days 11−13; the pH rises by about two units, from approximately day 7; the amount of total sugars, measured as %SS, shows the characteristic increase which, for the cultivar studied, is just under 2-fold. The results confirm that the pH and %SS measured for natural juices reflect the degree of ripening, mainly up to day 11; after that, variations are minimal in both quantities, hindering the determination of ripening stage. In addition, in the case of commercial juices, possible additives may significantly affect pH and %SS, thus reducing the ability to obtain information on the ripening stage (or quality) of the source fruits. Often, pH regulators (e.g., citric acid), sucrose, or other sweeteners are added so that pH and %SS are no longer a reflection of the ripening stage of the source fruit. Indeed, it has been observed (*28*) that, in the case of mango juice, the content of citric acid also contributes for the %SS value which, in such conditions, is no longer merely a measure of total sugars. Therefore, when citric acid is employed as a pH regulator,

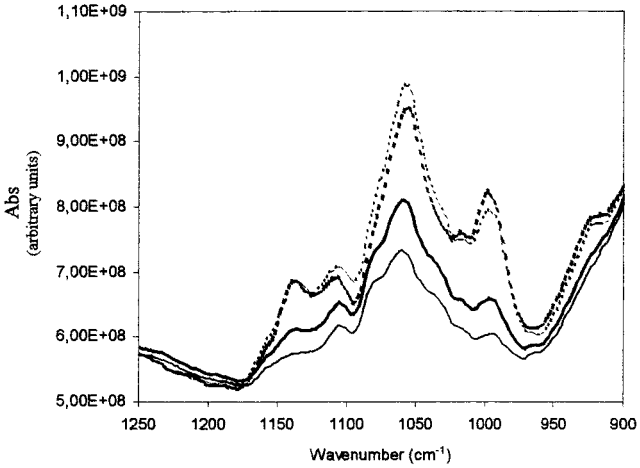

Figure 6. FTIR spectra of mango juices at different ripening stages (1250–900 cm^{-1}): day 1 (—), day 5 (**—**), day 9 (- - - -), and day 19 (·····).

significant changes are expected not only in pH but also in %SS. In these cases, evaluation of individual sugar contents (e.g., glucose and fructose, if sucrose is added) may still be used as an indicator of ripening stage. FTIR spectroscopy can potentially give information about the proportions of the three main sugars (sucrose, glucose, and fructose) and their variation with ripening. Indeed, the FTIR spectra of the mango juices collected at different ripening stages (**Figure 6**) show a tendency for total area increase, reflecting the increase in total sugars, as well as significant changes in spectral profile due to changes in the proportions of the three sugars.

Changes in Sugars Composition. The PCA of the FTIR spectra of the juices obtained as a function of ripening was carried out, and the resulting scores scatter plot is shown in **Figure 7a**. It is clear that the juices of days 1 to 5 are significantly separated from the remaining samples along the PC1 dimension. The PC1 loadings profile (**Figure 7b**) shows that the variations responsible for this separation correspond to variations in the sucrose spectral profile, as indicated by the strong similarity between the solid line in **Figure 7b** and the sucrose profile shown in **Figure 2b**. Indeed, it has been shown before (*2*, *3*, *5*) that the early stages of ripening mango ripening are accompanied by a significant increase in sucrose. For the Tommy Atkins cultivar, previous studies have shown that sucrose can increase up to 2-fold (*3*) during ripening, whereas glucose and fructose tend to decrease or fluctuate (*2*, *3*). Since citric acid is known to decrease drastically during the first stages of ripening (*3*, *4*), the possibility that this variation may contribute to the loadings plot in **Figure 7b** was considered. However, the fact that significant contributions are absent in regions of strong citric acid absorbtivity such as at 1180 or 1220 cm^{-1} indicates that the plot shown does not depend significantly on the variations in citric acid. The variability within the PC2 dimension is not as significant as that in PC1, as it accounts for only 2% of the total variability in the spectra. However, some distinction between juices of day 9 and those of the latest ripening stages (days 19 and 21) may be suggested from the plot (**Figure 7a**), probably reflecting mainly variations in the proportion of glucose and fructose.

The PLS1 regression model developed for the standard sugar solutions was applied to the first derivative functions of the mango juices spectra to quantify each of the three sugars at different ripening stages. Sucrose, glucose, and fructose were also quantified by specific enzymatic tests so that the accuracy of the predicted concentrations could be verified. The results are shown in **Table 3**. First, it should be noted that some

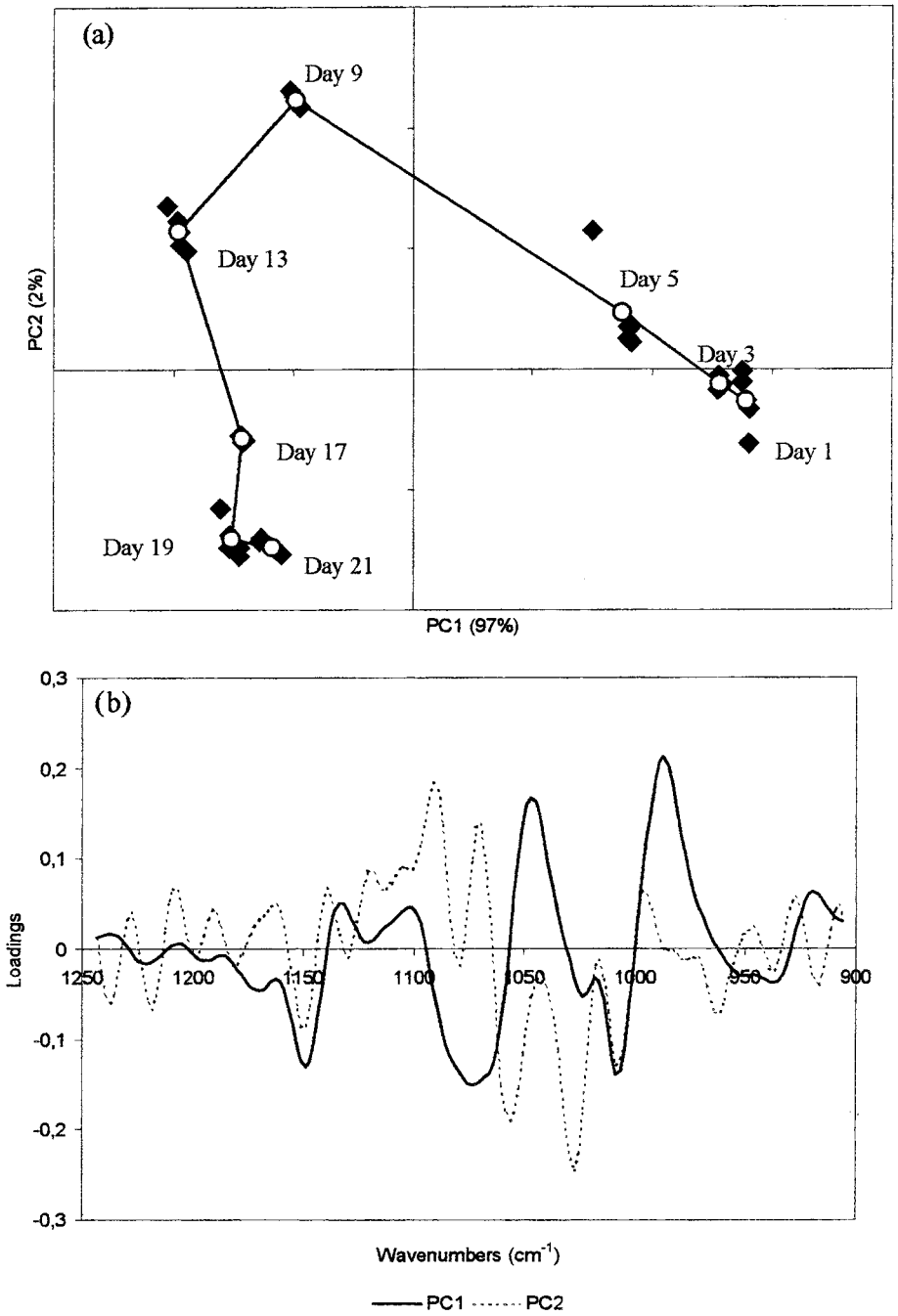

Figure 7. Results of the PCA of the mango juices FTIR spectra: (a) scores scatter plot; (b) loadings profile.

discrepancy occurs between FTIR and enzymatic results for sucrose and fructose in day 1. This may relate to the fact that the 5 replica spectra taken for day 1 juice show the highest dispersion (**Figure 7a**), therefore limiting the accuracy of the values obtained by PLS−FTIR. This shows how important replica reproducibility is for the success of this type of quantification. For days 3 to 9, both sets of data are in very good agreement for all sugars; for stages later than day 13, good agreement is shown for sucrose and fructose, but for glucose the concentrations determined enzymatically are consistently lower than those predicted by FTIR. This arises from the drastic glucose decrease, at later ripening stages, to concentration levels lower than those observed in previous studies (*3*, *4*). Since the glucose concentration levels found here (0.6−1.5 g/L) are well below the minimum glucose concentration present in the standard solutions used to build the PLS−FTIR model (3.0 g/L), such low concentrations could not be adequately predicted by this model. Therefore, the present PLS−FTIR model is able to predict sugar contents in mango juices with different ripening degrees with the following prediction errors (%RMSEP): 5.1% for sucrose (down to 1.3% if spectral dispersion in day 1 is improved); 6.7% for fructose (down to 4.8% if spectral dispersion in day 1 is improved); 8.0% for glucose until mid-stages of ripening, beyond which %RMSEP may reach about 25%.

The concentrations of the three sugars measured in the eight juice samples by PLS−FTIR are presented in **Figure 8** (full symbols), together with the enzymatic quantification results (open symbols). From the early stages of ripening, sucrose is the most abundant sugar, followed by fructose and glucose, as expected (*2*−*5*). Sucrose is seen to increase about 4-fold until day 13, and remains approximately constant at later stages, although a slight decreasing tendency is hinted as over-ripening is approached. Fructose shows very slight variations, whereas

Table 3. Concentrations (g/L) of the Three Sugars in Mango Juices at Different Ripening Stages: Predicted by PLS1 and Measured by Enzymatic Tests[a]

	glucose		fructose		sucrose	
ripening stage	PLS1	enzymatic	PLS1	enzymatic	PLS1	enzymatic
day 1	20.36 ± 1.00	19.34	34.28 ± 0.48	39.10	27.84 ± 0.40	38.15
day 3	18.27 ± 0.90	16.03	36.14 ± 0.51	35.70	31.48 ± 0.44	32.00
day 5	19.58 ± 0.96	17.13	37.17 ± 0.52	36.07	47.17 ± 0.66	47.63
day 9	11.71 ± 0.57	10.84	42.72 ± 0.60	43.64	98.59 ± 1.40	97.00
day 13	2.46 ± 0.12	0.58	42.68 ± 0.60	38.90	117.69 ± 1.65	118.02
day 17	2.49 ± 0.12	0.94	32.13 ± 0.45	32.67	109.40 ± 1.53	111.31
day 19	4.20 ± 0.21	1.29	26.40 ± 0.37	25.87	111.30 ± 1.56	110.80
day 21	4.46 ± 0.22	1.47	26.51 ± 0.37	n.d.	104.64 ± 1.46	n.d.

[a] The uncertainties of each PLS–FTIR predicted value are indicated; the precision of the enzymatic tests was found to be 1.5–1.6% for each type of test employed. n.d., not determined.

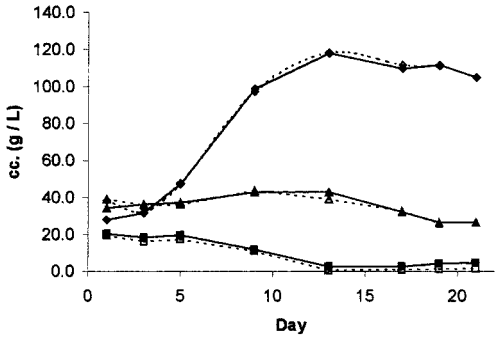

Figure 8. Variations of sucrose (◆), glucose (■), and fructose (▲) concentrations (g/L) as a function of ripening, measured by PLS–FTIR. The open symbols and dashed lines represent the results of the enzymatic tests. Error bars corresponding to the uncertainties indicated in **Table 3** are not represented because their magnitudes are of the order of the symbol sizes.

glucose decreases very markedly (about 30-fold, according to the enzymatic test results) until day 13. Glucose content remains low, despite hinting a slight increasing tendency as over-ripening is approached (days 19 and 21).

In conclusion, the PLS−FTIR method, calibrated by a triangular model of standard sugar solutions, has been shown to be suitable for the determination of sucrose, fructose, and glucose in mango juices obtained from fruits differing in ripening degrees. In the case of the variety studied (cv. Tommy Atkins), one of the most commercialized varieties, sucrose and fructose are accurately quantifiable throughout the ripening process, whereas glucose determination may carry a prediction error of up to 25% after day 9 (i.e., when the fruit is ready-to-eat). It is shown that the FTIR spectrum of a juice may, in this way, be used as a rapid indicator of ripening degree, particularly when pH and %SS of the fresh juice are not very sensitive to ripening degree (after the mid-stages of ripening) or when, in the case of commercial juices, they are affected by other factors e.g., addition of pH regulators or sweeteners.

The rapid determination of the ripening degree of mango fruits should be useful to establish suitable conditions for storage so that no over-ripening or other quality losses occur, particularly if long-term transportation is involved, as in the case of imported fruits. The same information is also important in regard to commercial juices, to establish if the source fruits had adequate ripening degrees (i.e., neither under- nor over-ripened). The present work refers to a particular mango variety, however, the method and model developed should be applicable to other varieties and possibly even to other fruits, as long as the sucrose/glucose/fructose proportion is sensitive to ripening degree and the sugar concentrations fall within the concentration ranges used in the sugar calibration model. In any case, for a new system (fruit of different variety or type) the trends of sugar variation should be characterized and the model concentration values should be checked and optimized.

ACKNOWLEDGMENT

We are grateful to Prof. D. Rutledge for his very helpful comments about this work.

LITERATURE CITED

(1) Lizada, C. Mango. In *Biochemistry of Fruit Ripening*; Seymour, G. B., Taylor, J. E., Tucker, G. A., Eds.; Chapman & Hall: London, 1993; pp 255−271.

(2) Medlicott, A. P.; Thompson, A. K. Analysis of sugars and organic acids in ripening mango fruits (*Mangifera indica* L. var. Keitt) by high performance liquid chromatography. *J. Sci. Food Agric.* **1985**, *36*, 561−566.

(3) Medlicott, A. P.; Reynolds, S. B.; Thompson, A. K. Effects of temperature on the ripening of mango fruit (*Mangifera indica* L. var. Tommy Atkins). *J. Sci. Food Agric.* **1986**, *37*, 469−474.

(4) Gil, A. M.; Duarte, I. F.; Delgadillo, I.; Colquhoun, I. J.; Casuscelli, F.; Humpfer, E.; Spraul, M. Study of the compositional changes of mango during ripening by nuclear magnetic resonance spectroscopy. *J. Agric. Food Chem.* **2000**, *48*, 1524−1536.

(5) Duarte, I.; Delgadillo, I.; Gil, A. M. An NMR study of the biochemistry of mango: the effects of ripening, storage conditions and microbial growth. In *Magnetic Resonance in Food Science − A view to the next century*; Webb, G. A., Belton, P. S., Gil, A. M., Delgadillo, I., Eds.; Royal Society of Chemistry: Cambridge, Great Britain, 2001; pp 259−266.

(6) Pomeranz, Y.; Meloan, C. E.; Refractometry and Polarimetry. In *Food Analysis*; Pomeranz, Y., Meloan, C. E., Eds.; Chapman & Hall: New York, 1994;pp 430−447.

(7) Corradini, C.; Canali, G.; Nicoletti, I. Application of HPAEC−PAD to carbohydrate analysis in food products and fruit juices. *Semin. Food Anal.* **1997**, *2*, 99−111.

(8) Cataldi, T. R. I.; Margiotta, G.; Zambonin, C. G. Determination of sugars and alditols in food samples by HPAEC with integrated pulsed amperometric detection using alkaline eluents containing barium or strontium ions. *Food Chem.* **1998**, *62*, 109−115.

(9) Lee, H. S.; Coates, G. A. Quantitative study of free sugars and myo-inositol in citrus juices by HPLC and a literature compilation. *J. Liq. Chromatogr. Relat. Technol.* **2000**, *23*, 2123−2141.

(10) Kemsley, E. K.; Holland, J. K.; Defernez, M.; Wilson, R. H. Detection of adulteration of raspberry purees using infrared spectroscopy and chemometrics. *J. Agric. Food Chem.* **1996**, *44*, 3864−3870.

(11) Defernez, M.; Wilson, R. H. Mid-infrared spectroscopy and chemometrics for determining the type of fruit used in jam. *J. Sci. Food Agric.* **1995**, *67*, 461−467.

(12) Wilson, R. H.; Tapp, H. S. Mid-infrared spectroscopy for food analysis: recent new applications and relevant developments in sample presentation methods. *Trends Anal. Chem.* **1999**, *18*, 85−93.

(13) Bellonmaurel, V.; Vallat, C.; Goffinet, D. Quantitative-analysis of individual sugars during starch hydrolysis by FT-IR/ATR spectrometry. 1. Multivariate calibration study-repeatability and reproducibility. *Appl. Spectrosc.* **1995**, *49*, 556−562.

(14) Coimbra, M. A.; Barros, A.; Rutledge, D. N.; Delgadillo, I. FTIR spectroscopy as a tool for the analysis of olive pulp cell-wall polysaccharide extracts. *Carbohydr. Res.* **1999**, *317*, 145−154.

(15) Kacuráková, M.; Wilson, R. H. Developments in mid-infrared FT-IR spectroscopy of selected carbohydrates. *Carbohydr. Polym.* **2001**, *44*, 291−303.

(16) Kemsley, E. K.; Wilson, R. H.; Poulter, G.; Day, L. L. Quantitative analysis of sugars solutions using a novel fiber-optic-based sapphire ATR accessory. *Appl. Spectrosc.* **1993**, *47*, 1651−1654.

(17) Kellner, R.; Lendl, B.; Wells, I.; Worsfold, P. J. Comparison and univariate and multivariate strategies for the determination of sucrose in fruit juices by automated flow injection analysis with Fourier transform infrared detection. *Appl. Spectrosc.* **1997**, *51*, 227−235.

(18) Rambla, F. J.; Garrigues, S.; Ferrer, N.; de la Guardia, M. Simple partial least squares-attenuated total reflectance Fourier transform infrared spectrometric method for the determination of sugars in fruit juices and soft drinks using aqueous standards. *Analyst* **1998**, *123*, 277−281.

(19) Cadet, F.; Offmann, B. Direct spectroscopic sucrose determination of raw sugar cane juices. *J. Agric. Food Chem.* **1997**, *45*, 166−171.

(20) Cadet, F. Measurement of sugar content by multidimensional analysis and mid-infrared spectroscopy. *Talanta* **1999**, *48*, 867−875.

(21) Garrigues, S.; Rambla, F. J.; de la Guardia, M. Comparative study of reflectance cells for PLS−FTIR determination of sugars in soft drinks. *Fresenius' J. Anal. Chem.* **1998**, *362*, 137−140.

(22) Tewari, J.; Joshi, M.; Gupta, A.; Mehrotra, R.; Chandra, S. Determination of sugars and organic acid concentration in apple juices using infrared spectroscopy. *J. Sci. Ind. Res.* **1999**, *58*, 19−24.

(23) Hulme, A. C. The Mango. In *The Biochemistry of Fruits and their Products*; Hulme, A. C., Ed.; Academic Press: London, 1971; pp 233−254.

(24) Taylor, R. B. Ingredients. In *Chemistry and Analysis of Soft Drinks and Fruit Juices*; Ashurst, P. R., Ed.; Sheffield Academic Press: Sheffield, England, 1998; pp 20−21.

(25) Jolliffe, I. T. *Principal Component Analysis*. Springer: New York, 1986.

(26) Geladi, P.; Kowalski, B. R. Partial least-squares regression: a tutorial. *Anal. Chim. Acta* **1986**, *185*, 1−17.

(27) Savitsky, A.; Golay, M. J. E. Smoothing and differentiation of data by simplified least squares procedures. *Anal. Chem.* **1964**, *36*, 1627−1639.

(28) Duarte, I.; Barros, A.; Delgadillo, I.; Spraul, M.; Humpfer, E.; Gil, A. M. Unpublished results.

Received for review November 30, 2001. Revised manuscript received February 28, 2002. Accepted March 4, 2002.

JF011575Y